ISSN 1674-1056
http://cpb.iphy.ac.cn
http://iopscience.iop.org/cpb
中国物理 B
Chinese Physics
中国物理 Chinese Physics B

420 nm thick $CH_3NH_3PbI_{3-x}Br_x$ capping layers for efficient TiO_2 nanorod array perovskite solar cells

Long Li(李龙), Cheng-Wu Shi(史成武), Xin-Lian Deng(邓新莲), Yan-Qing Wang(王艳青), Guan-Nan Xiao(肖冠南), Ling-Ling Ni(倪玲玲)
Citation: Chin. Phys. B . 2018, 27(1): 018804. **doi:** 10.1088/1674-1056/27/1/018804

Journal homepage: http://cpb.iphy.ac.cn; http://iopscience.iop.org/cpb

What follows is a list of articles you may be interested in

Efficient design of perovskite solar cell using mixed halide and copper oxide

Navneet kour, Rajesh Mehra, Chandni
Chin. Phys. B . 2018, 27(1): 018801. **doi:** 10.1088/1674-1056/27/1/018801

Promise of commercialization:carbon materials for low-cost perovskite solar cells

Yu Cai(蔡宇), Lusheng Liang(梁禄生), Peng Gao(高鹏)
Chin. Phys. B . 2018, 27(1): 018805. **doi:** 10.1088/1674-1056/27/1/018805

O_3 fast and simple treatment-enhanced p-doped in Spiro-MeOTAD for CH_3NH_3I vapor-assisted processed $CH_3NH_3PbI_3$ perovskite solar cells

En-Dong Jia(贾恩东), Xi Lou(娄茜), Chun-Lan Zhou(周春兰), Wei-Chang Hao(郝维昌), Wen-Jing Wang(王文静)
Chin. Phys. B . 2017, 26(6): 068803. **doi:** 10.1088/1674-1056/26/6/068803

Simulation design of P-I-N-type all-perovskite solar cells with high efficiency

Hui-Jing Du(杜会静), Wei-Chao Wang(王韦超), Yi-Fan Gu(顾一帆)
Chin. Phys. B . 2017, 26(2): 028803. **doi:** 10.1088/1674-1056/26/2/028803

Device simulation of lead-free $CH_3NH_3SnI_3$ perovskite solar cells with high efficiency

Hui-Jing Du(杜会静), Wei-Chao Wang(王韦超), Jian-Zhuo Zhu(朱键卓)
Chin. Phys. B . 2016, 25(10): 108802. **doi:** 10.1088/1674-1056/25/10/108802

SPECIAL TOPIC — New generation solar cells

420 nm thick $CH_3NH_3PbI_{3-x}Br_x$ capping layers for efficient TiO_2 nanorod array perovskite solar cells*

Long Li(李龙), Cheng-Wu Shi(史成武)†, Xin-Lian Deng(邓新莲), Yan-Qing Wang(王艳青), Guan-Nan Xiao(肖冠南), and Ling-Ling Ni(倪玲玲)

School of Chemistry and Chemical Engineering, Anhui Province Key Laboratory of Advanced Catalytic Materials and Reaction Engineering, Hefei University of Technology, Hefei 230009, China

(Received 23 September 2017; revised manuscript received 16 November 2017; published online 13 December 2017)

The rutile TiO_2 nanorod arrays with 240 nm in length, 30 nm in diameter, and 420 μm^{-2} in areal density were prepared by the hydrothermal method to replace the typical 200–300 nm thick mesoporous TiO_2 thin films in perovskite solar cells. The $CH_3NH_3PbI_{3-x}Br_x$ capping layers with different thicknesses were obtained on the TiO_2 nanorod arrays using different concentration PbI_2·DMSO complex precursor solutions in DMF and the photovoltaic performances of the corresponding solar cells were compared. The perovskite solar cells based on 240 nm long TiO_2 nanorod arrays and 420 nm thick $CH_3NH_3PbI_{3-x}Br_x$ capping layers showed the best photoelectric conversion efficiency (PCE) of 15.56% and the average PCE of $14.93 \pm 0.63\%$ at the relative humidity of 50%–54% under the illumination of simulated AM 1.5 sunlight (100 mW·cm^{-2}).

Keywords: rutile TiO_2 nanorod array, $CH_3NH_3PbI_{3-x}Br_x$, capping layer, perovskite solar cell

PACS: 88.40.H−, 88.40.hj, 84.60.Jt **DOI:** 10.1088/1674-1056/27/1/018804

1. Introduction

Organometal halide perovskite solar cells ($CH_3NH_3PbX_3$, $X = $ I, Br, Cl) have drawn tremendous attention due to their excellent photovoltaic performance such as long electron–hole diffusion length, strong optical absorption, tunable band gaps, and simple manufacturing process.[1–7] The thicknesses of the perovskite thin films strongly affect their absorbance and further influence the photovoltaic performance of the corresponding solar cells. Snaith[8] fabricated the perovskite solar cells with 200 nm thick $CH_3NH_3PbI_{3-x}Cl_x$ capping layer and 260 nm thick mesoporous TiO_2 thin film by a one-step solution method, and obtained the photoelectric conversion efficiency (PCE) of 8.44%. Park[9] prepared a ∼200 nm thick $CH_3NH_3PbI_3$ capping layer using the 1.0 M PbI_2precursor solution by a two-step solution method and the corresponding perovskite solar cells with 220 nm thick mesoporous TiO_2 thin film achieved the PCE of 12.5%. Seok[10] prepared a 200 nm thick perovskite capping layer using the 0.8 M $CH_3NH_3PbI_{3-x}Br_x$ precursor solution by a one-step solution method and the corresponding perovskite solar cells with 200 nm thick mesoporous TiO_2 thin film exhibited the PCE of 15.9%. Mhaisalkar and Park[11] studied the influence of the rutile TiO_2 nanorod array with lengths of 560 nm, 920 nm, and 1580 nm on the PCE of the corresponding perovskite solar cells and found that 560 nm long rutile TiO_2 nanorod arrays gave the best PCE of 9.4%. Li, Xie, and Wang[12] assembled the perovskite solar cells with 200 nm long TiO_2 nanorod array and 100 nm thick $CH_3NH_3PbI_3$ capping layer using the 1.3 M $CH_3NH_3PbI_3$ precursor solution, the corresponding perovskite solar cells achieved the best PCE of 18.22%. Although the perovskite solar cells with 200–300 nm thick mesoporous TiO_2 thin films and 100–200 nm thick $CH_3NH_3PbI_3$ capping layers have been widely investigated, the TiO_2 nanorod array perovskite solar cells with high thickness $CH_3NH_3PbI_{3-x}Br_x$ capping layers have been rarely reported.

In this work, the rutile TiO_2 nanorod arrays of 240 nm in length, 30 nm in diameter, and 420 μm^{-2} in areal density were prepared via hydrothermal method using an aqueous grown solution composed by 38 mW titanium isopropoxide and 6 M hydrochloric acid at 170 °C for 75 min. 290 nm, 360 nm, and 420 nm thick $CH_3NH_3PbI_{3-x}Br_x$ capping layers were obtained on the TiO_2 nanorod arrays using 1.3 M, 1.5 M, and 1.7 M PbI_2·DMSO complex precursor solutions in DMF, respectivley. The influence of the $CH_3NH_3PbI_{3-x}Br_x$ capping layer thickness on the photovoltaic performance of the corresponding TiO_2 nanorod array perovskite solar cells was compared.

2. Experimental section

2.1. Preparation of the $CH_3NH_3PbI_{3-x}Br_x$ capping layers

70 μL PbI_2·DMSO complex precursor solutions with 1.3 M, 1.5 M, 1.7 M in DMF[13] were dropped on TiO_2 nanorod arrays and spin-coated at 3000 rpm for 20 s. Immediately, 100 μL, 0.465 M methylammonium halide

*Project supported by the National Natural Science Foundation of China (Grant Nos. 51472071 and 51272061) and Talent Project of Hefei University of Technology, China (Grant Nos. 75010-037004 and 75010-037003).

†Corresponding author. E-mail: shicw506@foxmail.com; shicw506@hfut.edu.cn

© 2018 Chinese Physical Society and IOP Publishing Ltd

mixture of $CH_3NH_3I/CH_3NH_3Br = 85/15$ (molar ratio) in isopropanol[13] was dropped. After waiting for 20 s, the spin-coater was started to remove the residual methylammonium halide mixture solution and the parameters of the spin-coating procedure were 5000 rpm and 30 s. Subsequently, these $CH_3NH_3PbI_{3-x}Br_x$ capping layers were heated on a pre-heated hot plate in the glove box with the relative humidity of 10%–15% and the annealing temperature and time were 110 °C and 30 min, respectively. Moreover, the spin-coater was immediately started (after waiting for 0 s) and these $CH_3NH_3PbI_{3-x}Br_x$ capping layers were obtained to analyze the complete conversion of PbI_2·DMSO and the content of residual PbI_2 for comparisons.

2.2. Preparation of the rutile TiO_2 nanorod arrays and fabrication of perovskite solar cells

The rutile TiO_2 nanorod arrays were prepared by hydrothermal method similar to that in our previous reports.[14,15] The aqueous grown solution was composed of 38 mW titanium isopropoxide and 6 M hydrochloric acid. The growth temperature and time were 170 °C and 75 min, respectivley. The rutile TiO_2 nanorod arrays were annealed at 300 °C for 30 min in air prior to use.[11] The preparation of the 60 nm thick TiO_2 compact layer, spiro-OMeTAD layer, 60 nm thick gold electrode and the fabrication of perovskite solar cells were the same as in our previous reports.[13,14]

2.3. Characterization

The characterization with field emission scanning electron microscopy (FE-SEM, Sirion200, FEI), x-ray diffraction (XRD, D/MAX2500V, Rigaku, Japan), ultraviolet–visible spectroscopy (UV–Vis, U-3900H, Hitachi, Japan), ultraviolet–visible–near infrared spectroscopy (UV–Vis–NIR, U-3900H, Hitachi, Japan), electrochemical impedance spectroscopy (EIS, electrochemical workstation, Shanghai), and energy dispersive x-ray spectroscopy (EDS, JSM-6490LV, Japan) were identical to that in our previous reports.[13–15] The photovoltaic performance of the perovskite solar cells was measured by a solar simulator (Oriel, Newport, USA) with a source meter (Keithley 2420) controlled by Testpoint software under the illumination of simulated AM 1.5 sunlight (100 $mW{\cdot}cm^{-2}$). The irradiation intensity was calibrated with the standard crystalline silicon solar cell (Oriel, Newport, USA). The black and opaque film with the square aperture (3 mm × 3 mm) adhered on FTO and the active area of 0.09 cm^2 were defined and the PCE measurements were carried out in atmosphere air ambient with the relative humidity of 50%–54%.

3. Results and discussion

3.1. Microstructure, crystal phase, and optical absorption of the TiO_2 nanorod arrays

Figure 1 shows the microstructure, XRD pattern, and UV–Vis spectrum of the TiO_2 nanorod array on 60 nm thick TiO_2 compact layer and SnO_2:F transparent conductive glass (FTO). From Figs. 1(a) and 1(b), it is found that the TiO_2 nanorod arrays have the length of 240 nm, the diameter of 30 nm, and the areal density of 420 μm^{-2}. The 240 nm length is similar to the typical 200–300 nm thickness of the mesoporous TiO_2 thin films in perovskite solar cells.[16,17] Compared with the planar perovskite solar cell without mesoporous TiO_2 thin films, the introduction of the TiO_2 nanorod array can improve the charge separation in the interface of perovskite/TiO_2.[14] As shown in Fig. 1(c), in addition to the strong diffraction peaks of FTO, the weak peaks appearing at $2\theta = 36.1°$ and 62.8° match well with the spacings of (101) and (002) planes of the tetragonal rutile phase, and the (101) plane is the preferred orientation of the TiO_2 nanorod arrays.[15] And the intensities of the diffraction peaks of TiO_2 increase with the increase of the hydrothermal growth time.[18] As shown in Fig. 1(d), the absorption onset of the TiO_2 nanorod arrays is 353 nm and nearly no obvious absorbance can be observed from 400 nm to 800 nm.

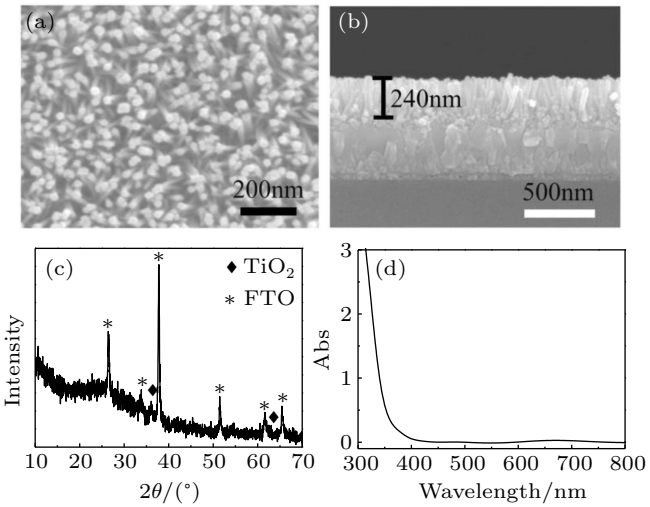


Fig. 1. TiO_2 nanorod array: (a) surface SEM image, (b) cross-sectional SEM image, (c) XRD pattern, (d) UV–Vis absorption spectrum.

3.2. Crystal phase, morphology, and optical absorption of the $CH_3NH_3PbI_{3-x}Br_x$ capping layers

Figure 2 shows the XRD patterns of the $CH_3NH_3PbI_{3-x}Br_x$ capping layers using 1.3 M, 1.5 M, and 1.7 M PbI_2·DMSO complex precursor solutions after waiting for 0 s and 20 s. The $CH_3NH_3PbI_{3-x}Br_x$ capping layers at 0 s all exhibit the weak diffraction peaks of PbI_2,[19] while the diffraction peaks of PbI_2 do not appear at 20 s and the diffraction peaks of $CH_3NH_3PbI_{3-x}Br_x$ appear at $2\theta = 14.15°$, 20.07°, 23.54°, 24.60°, 28.50°, 31.97°, 40.79°, and 43.33°.[13,14] The result demonstrates that PbI_2·DMSO does not completely convert to $CH_3NH_3PbI_{3-x}Br_x$ at 0 s and the pure phase $CH_3NH_3PbI_{3-x}Br_x$ capping layers can be obtained at 20 s.

Figure 3 displays the cross-sectional and surface SEM images of the $CH_3NH_3PbI_{3-x}Br_x$ capping layers using 1.3 M, 1.5 M, and 1.7 M PbI_2·DMSO complex precursor solutions

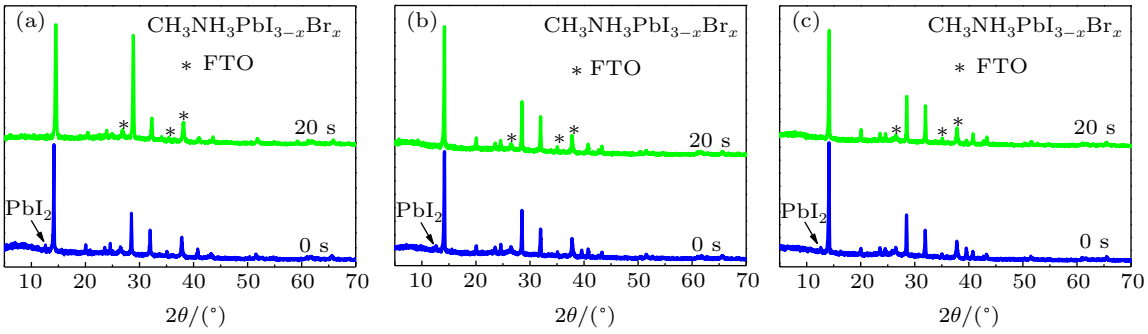


Fig. 2. (color online) XRD patterns of the $CH_3NH_3PbI_{3-x}Br_x$ capping layers using (a) 1.3 M, (b) 1.5 M, (c) 1.7 M PbI_2·DMSO complex precursor solutions after waiting for 0 s and 20 s.

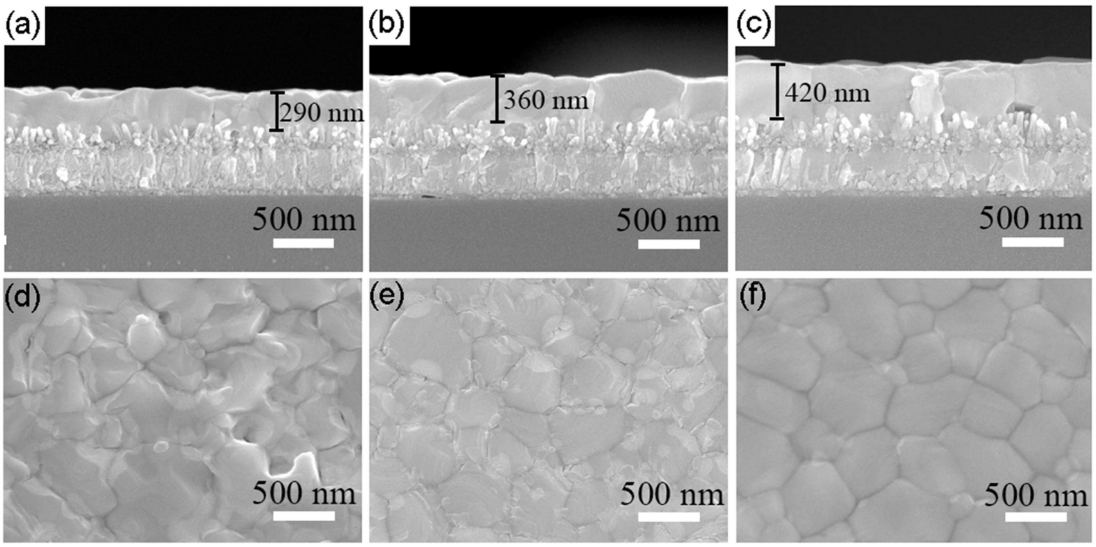


Fig. 3. Cross-sectional and surface SEM images of the $CH_3NH_3PbI_{3-x}Br_x$ capping layers using (a), (d) 1.3 M, (b), (e) 1.5 M, and (c), (f) 1.7 M PbI_2·DMSO complex precursor solutions.

after waiting for 20 s. From Figs. 3(a)–3(c), the thicknesses of the $CH_3NH_3PbI_{3-x}Br_x$ capping layers are 290 nm of 1.3 M, 360 nm of 1.5 M, and 420 nm of 1.7 M and increase with the PbI_2·DMSO concentration. And the total thicknesses of the $CH_3NH_3PbI_{3-x}Br_x$ absorbing layers reach 530 nm of 1.3 M, 600 nm of 1.5 M, and 660 nm of 1.7 M. From Figs. 3(d)–3(f), the $CH_3NH_3PbI_{3-x}Br_x$ capping layers with the thicknesses of 360 nm and 420 nm have more uniform grain sizes, less grain boundaries, and more smooth surfaces than that of 290 nm, and the grain size of perovskite is 500–800 nm in the 420 nm thick $CH_3NH_3PbI_{3-x}Br_x$ capping layer. The EDS analysis reveals that the chemical composition of the 420 nm thick $CH_3NH_3PbI_{3-x}Br_x$ capping layer is the atomic ratio of Pb : I : Br = 1 : 3.18 : 0.24. Combined with the results of XRD, SEM, and EDS, the Br-doped $CH_3NH_3PbI_{3-x}Br_x$ capping layers with high thickness of 420 nm are successfully obtained. It is worthwhile to note that the concentration of the PbI_2·DMSO complex precursor saturated solution is $\sim$ 1.7 M, the $CH_3NH_3PbI_{3-x}Br_x$ capping layers with thicknesses lager than 420 nm are not prepared in this paper.

Figure 4 exhibits the UV–Vis–NIR absorption spectra of the $CH_3NH_3PbI_{3-x}Br_x$ capping layers using 1.3 M, 1.5 M, and 1.7 M PbI_2·DMSO complex precursor solutions after waiting for 20 s. The absorption onsets of the $CH_3NH_3PbI_{3-x}Br_x$ capping layers are all 780 nm and the absorbance in the range of 500–800 nm increases with the increase of the PbI_2·DMSO complex precursor solution concentration and the $CH_3NH_3PbI_{3-x}Br_x$ capping layer thickness, which is accordance with the result of SEM in Fig. 3.

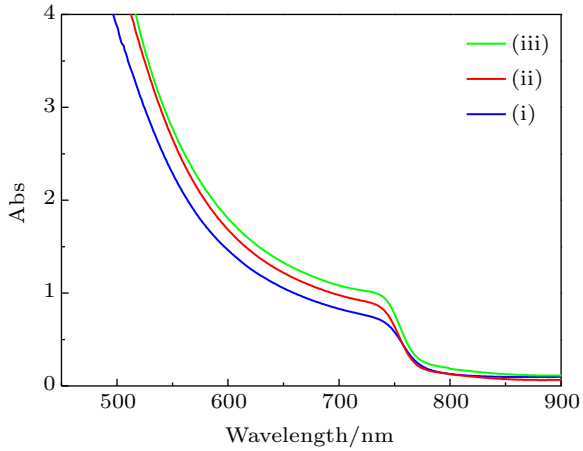


Fig. 4. (color online) UV–Vis–NIR absorption spectra of $CH_3NH_3PbI_{3-x}Br_x$ capping layers using (i) 1.3 M, (ii) 1.5 M, and (iii) 1.7 M PbI_2·DMSO complex precursor solutions.

3.3. Photovoltaic performance of the TiO_2 nanorod array $CH_3NH_3PbI_{3-x}Br_x$ solar cells

Table 1 lists the photovoltaic performance parameters of the TiO_2 nanorod array perovskite solar cells with the different thicknesses of $CH_3NH_3PbI_{3-x}Br_x$ capping layers and the photocurrent–photovoltage characteristics, and the incident photon-to-electron conversion efficiency (IPCE) spectra of the corresponding champion solar cells are shown in Fig. 5. With the increase of the $CH_3NH_3PbI_{3-x}Br_x$ capping layer thickness from 290 nm to 360 nm and 420 nm, the short-circuit photocurrent density (J_{sc}) and open-circuit voltage (V_{oc}) increase from 19.91 ± 3.81 mA·cm^{-2} and 0.81 ± 0.03 V of 290 nm, to 20.93 ± 0.66 mA·cm^{-2} and 0.91 ± 0.03 V of 360 nm, 21.56 ± 1.10 mA·cm^{-2} and 0.98 ± 0.04 V of 420 nm. The increase of J_{sc} should be related to the thickness and absorbance increases of the $CH_3NH_3PbI_{3-x}Br_x$ capping layers. From the IPCE spectra in Fig. 5(b), the integrated J_{sc} of the corresponding champion solar cells (1.3 M, 1.5 M, 1.7 M) are 20.42 mA cm^{-2}, 20.43 mA cm^{-2}, and 21.33 mA cm^{-2}, which are in close agreement with the measured values. When the thickness of the $CH_3NH_3PbI_{3-x}Br_x$ capping layers is increased, the quantity of conduction band electrons injecting from $CH_3NH_3PbI_{3-x}Br_x$ to TiO_2 increases under the illumination and the level of the TiO_2 conduction band up-shifts.

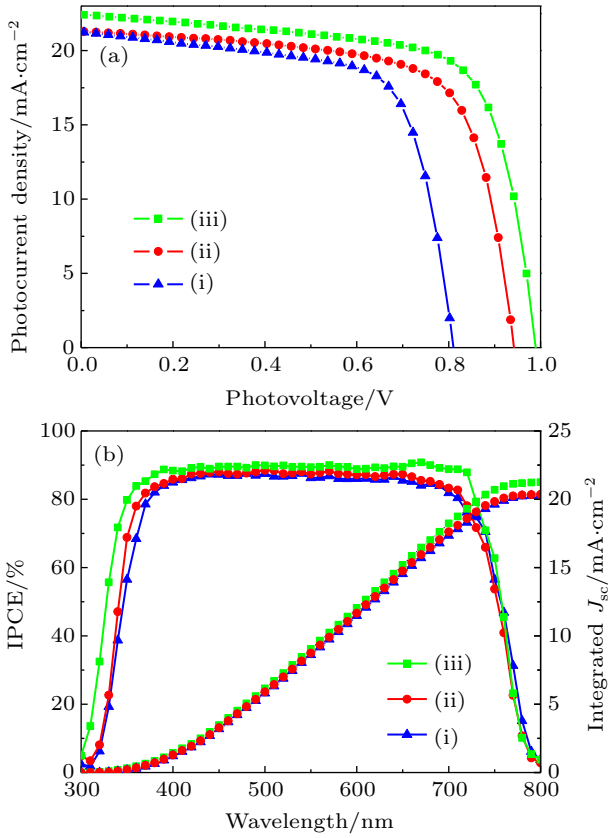


Fig. 5. (color online) (a) Photocurrent–photovoltage characteristics of the TiO_2 nanorod array perovskite solar cells with (i) 290 nm, (ii) 360 nm, and (iii) 420 nm thick $CH_3NH_3PbI_{3-x}Br_x$ capping layers and (b) the corresponding IPCE spectra.

Table 1. The photovoltaic performance parameters of TiO_2 nanorod array perovskite solar cells using 1.7 M, 1.5 M, and 1.3 M PbI_2·DMSO complex precursor solutions.

PbI_2·DMSO concentration	$CH_3NH_3PbI_{3-x}Br_x$ capping layer thickness/nm		V_{oc}/V	J_{sc}/mA·cm^{-2}	FF	PCE/%
1.7 M	420	best	0.99	22.42	0.70	15.56
		average[a]	0.98 ± 0.04	21.56 ± 1.10	0.70 ± 0.04	14.93 ± 0.63
1.5 M	360	best	0.94	21.28	0.69	13.89
		average[a]	0.91 ± 0.03	20.93 ± 0.66	0.65 ± 0.05	12.45 ± 1.44
1.3 M	290	best	0.81	21.23	0.69	11.80
		average[a]	0.81 ± 0.03	19.91 ± 3.81	0.67 ± 0.05	10.77 ± 2.03

[a] Average of 6 solar cells.

The grain boundary energy should be minimized and the charge transportation can be improved because the $CH_3NH_3PbI_{3-x}Br_x$ capping layers with the thicknesses of 360 nm and 420 nm have more uniform grain sizes, less grain boundaries, and more smooth surface than that of 290 nm.[20] The V_{oc} of 360 nm and 420 nm is higher than that of 290 nm thick $CH_3NH_3PbI_{3-x}Br_x$ capping layer. Therefore, the perovskite solar cell based on the combination of 420 nm thick $CH_3NH_3PbI_{3-x}Br_x$ capping layers and 240 nm long rutile TiO_2 nanorod arrays achieves the best PCE of 15.56% with J_{sc} of 22.42 mA·cm^{-2}, V_{oc} of 0.99 V, and FF of 0.70 and the average PCE of 14.93 ± 0.63% with J_{sc} of 21.56 ± 1.10 mA·cm^{-2}, V_{oc} of 0.98 ± 0.04 V, and FF of 0.70 ± 0.04 at the relative humidity of 50%–54% under the illumination of simulated AM 1.5 sunlight (100 mW·cm^{-2}).

3.4. EIS analysis of the TiO_2 nanorod array perovskite solar cells with different $CH_3NH_3PbI_{3-x}Br_x$ capping layer thicknesses

The effect of the $CH_3NH_3PbI_{3-x}Br_x$ capping layer thickness on the photovoltaic performance of perovskite solar cells can be further investigated by analyzing the corresponding EIS.[21–25] Figure 6 shows the Nyquist plots of the perovskite solar cells with different $CH_3NH_3PbI_{3-x}Br_x$ capping layer thicknesses, and the corresponding fitted data by an equivalent circuit R_s (R_{cr} CPE) are listed in Table 2. The serial resistance R_s describes the resistance of the FTO and Au electrode, R_{cr} is the charge recombination resistance of the electrons in the TiO_2 conduction band and the holes in the

$CH_3NH_3PbI_{3-x}Br_x$ thin film, and Y_0 and n represent the capacitance and the contact extent of the $TiO_2/CH_3NH_3PbI_{3-x}Br_x$ thin film interface. Therefore, the arc difference in the Nyquist plots (Fig. 6) should be derived from the thickness difference of the $CH_3NH_3PbI_{3-x}Br_x$ thin films. From Table 2, with the increase of the $CH_3NH_3PbI_{3-x}Br_x$ capping layer thickness from 290 nm to 360 nm and 420 nm, R_{cr} and n both increase from 243.8 Ω, 0.87 to 634.2 Ω, 0.89 and 687.3 Ω and 0.98, respectively, while Y_0 decreases from 2.72×10^{-7} F·s^{n-1} to 1.23×10^{-7} F·s^{n-1} and 0.43×10^{-7} F·s^{n-1}. The increasing R_{cr} and n can be attributed to the more uniform grain sizes, less grain boundaries, and smoother surfaces with the increasing $CH_3NH_3PbI_{3-x}Br_x$ capping layer thickness which suppress the charge recombination of the electrons in the TiO_2 conduction band and the holes in the $CH_3NH_3PbI_{3-x}Br_x$ thin film and are benefit to better charge transporting in the $CH_3NH_3PbI_{3-x}Br_x$ thin film; this is consistent well with the SEM image results of the $CH_3NH_3PbI_{3-x}Br_x$ capping layers. On the other hand, the increasing $CH_3NH_3PbI_{3-x}Br_x$ capping layer thickness also leads to a decrease of the capacitance which causes the decrease of Y_0. The results of R_{cr} and Y_0 are in accordance with the increasing J_{sc} and V_{oc} of the corresponding perovskite solar cells.

Table 2. Parameters obtained by fitting the experimental spectra with the equivalent circuit R_s (R_{cr} CPE).

$CH_3NH_3PbI_{3-x}Br_x$ capping layer thickness/nm	R_s/Ω	R_{cr}/Ω	$Y_0/10^{-7}$ F·s^{n-1}	n
290	11.15	243.8	2.72	0.87
360	12.62	634.2	1.23	0.89
420	12.83	687.3	0.43	0.98

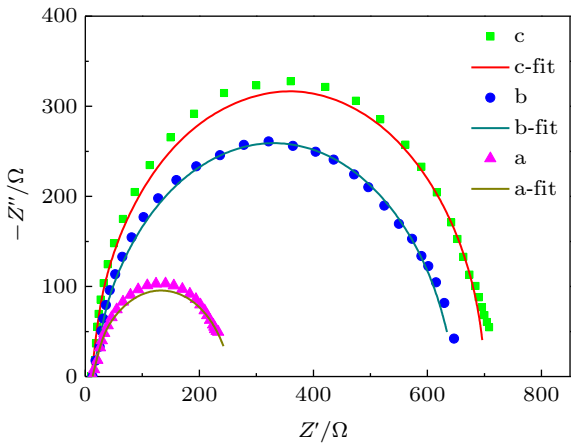


Fig. 6. (color online) Nyquist plots of the TiO_2 nanorod array perovskite solar cells with 290 nm (a, a-fit), 360 nm (b, b-fit), and 420 nm (c, c-fit) thick $CH_3NH_3PbI_{3-x}Br_x$ capping layers.

4. Conclusion

The rutile TiO_2 nanorod arrays with 240 nm in length, 30 nm in diameter, and 420 μm^{-2} in areal density were prepared via a hydrothermal method using an aqueous grown solution consisted of 38 mW titanium isopropoxide and 6 M hydrochloric acid at 170 °C for 75 min. 290 nm, 360 nm, and 420 nm thick $CH_3NH_3PbI_{3-x}Br_x$ capping layers were successfully obtained on the TiO_2 nanorod arrays using 1.3 M, 1.5 M, and 1.7 M PbI_2·DMSO complex precursor solutions in DMF and the corresponding $CH_3NH_3PbI_{3-x}Br_x$ solar cells presented the best PCE of 11.80%, 13.89%, and 15.56% and the average PCE of $10.77\pm2.03\%$, $12.45\pm1.44\%$, and $14.93\pm0.63\%$ at the relative humidity of 50%–54% under the illumination of simulated AM 1.5 sunlight (100 mW·cm^{-2}).

References

[1] Yin W J, Shi T and Yan Y 2014 *Adv. Mater.* **26** 4653
[2] Stranks S D, Eperon G E, Grancini G, Menelaou C, Alcocer M J P, Leijtens T, Herz L M, Petrozza A and Snaith H J 2013 *Science* **342** 341
[3] Xiao J Y, Shi J J, Liu H B, Xu Y Z, Lv S T, Luo Y H, Li D M, Meng Q B and Li Y L 2015 *Adv. Energy Mater.* **5** 1401943
[4] Lv S T, Han L Y, Xiao J Y, Zhu L F, Shi J J, Wei H Y, Xu Y Z, Dong J, Xu X, Li D M, Wang S R, Luo Y H, Meng Q B and Li X G 2014 *Chem. Commun.* **50** 6931
[5] Liu P, Yang B, Liu G, Wu R, Zhang C, Wan F, Li S, Yang J, Gao Y and Zhou C 2017 *Chin. Phys. B* **26** 058401
[6] Li J, Zhao C, Zhang H, Tong J, Zhang P, Yang C, Xia Y and Fan D 2016 *Chin. Phys. B* **25** 028402
[7] Du H J, Wang W C and Gu Y F 2017 *Chin. Phys. B* **26** 028803
[8] Snaith H J, Abate A, Ball J M, Eperon G E, Leijtens T, Noel N K, Stranks S D, Wang J T W, Wojciechowski K and Zhang W 2014 *J. Phys. Chem. Lett.* **5** 1511
[9] Kim H S and Park N G 2014 *J. Phys. Chem. Lett.* **5** 2927
[10] Jeon N J, Noh J H, Kim Y C, Yang W S, Ryu S and Seok S I 2014 *Nat. Mater.* **13** 897
[11] Kim H S, Lee J W, Yantara N, Boix P P, Kulkarni S A, Mhaisalkar S, Grätzel M and Park N G 2013 *Nano Lett.* **13** 2412
[12] Li X, Dai S, Zhu P, Deng L, Xie S, Cui Q, Chen H, Wang N and Lin H 2016 *ACS Appl. Mater. Inter.* **8** 21358
[13] Lu M, Shi C, Ma C, Li N, Li L and Xiao G 2017 *J. Mater. Sci: Mater. Electron.* **28** 5603
[14] Xiao G, Shi C, Zhang Z, Li N and Li L 2017 *J. Solid State Chem.* **249** 169
[15] Zhang Z, Shi C, Chen J, Xiao G and Li L 2017 *Appl. Surf. Sci.* **410** 8
[16] Jeon N J, Noh J H, Yang W S, Kim Y C, Ryu S, Seo J and Seok S I 2015 *Nature* **517** 476
[17] Yang W S, Noh J H, Jeon N J, Kim Y C, Ryu S, Seo J and Seok S I 2015 *Science* **348** 1234
[18] Chen J, Shi C, Zhang Z, Xiao G, Shao Z and Li N 2017 *Acta Phys. -Chim. Sin.* **33** 2029
[19] Jo Y, Oh K S, Kim M, Kim K H, Lee H, Lee C W and Kim D S 2016 *Adv. Mater. Interfaces* **3** 1500768
[20] Tu Y, Wu J, Lan Z, He X, Dong J, Jia J, Guo P, Lin J, Huang M and Huang Y 2017 *Sci. Rep.* **7** 44603
[21] Zhang J, Shi C, Chen J, Wang Y and Li M 2016 *J. Solid State Chem.* **238** 223
[22] Xu X, Zhang H, Shi J, Dong J, Luo Y, Li D and Meng Q 2015 *J. Mater. Chem. A* **3** 19288
[23] Shi J J, Xu X, Li D M and Meng Q B 2015 *Small* **11** 2472
[24] Shi J J, Luo Y H, Wei H Y, Luo J H, Dong J, Lv S T, Xiao J Y, Xu Y Z, Zhu L F, Xu X, Wu H J, Li D M and Meng Q B 2014 *ACS Appl. Mater. Inter.* **6** 9711
[25] Liu C, Qiu Z, Meng W, Chen J, Qi J, Dong C and Wang M 2015 *Nano Energy* **12** 59